Design considerations for a strontium optical frequency standard

I. Courtillot, A. Quessada, R.P. Kovacich, J-J. Zondy,
A. Landragin, A. Clairon and P. Lemonde
BNM-SYRTE, 61 Av. de l'observatoire, 75014 Paris, France
email: irene.courtillot@obspm.fr

Abstract

We present the work carried out in the scope of making an optical clock with cold strontium atoms at BNM-SYRTE. To load a magneto-optical trap (MOT), an atomic beam is slowed with a Zeeman slower using the cycling transition $^1S_0 \rightarrow {}^1P_1$ at 461 nm. We measured a flux of 2.3×10^{11} atoms/s slowed below 50 m/s. To generate the 461 nm laser, the frequencies of a Nd:YAG and diodes at 813 nm are summed in a KTP crystal. We obtained 115 mW of blue light corresponding to an efficiency of $2.7 \times 10^{-3} W/W^2$. We then present the set up used to realize a low frequency noise laser at 689 nm. An extended cavity diode laser is locked to a Fabry-Perot cavity of high finesse. For long term stabilisation, a Ramsey-Bordé interferometer will be used.

1 Introduction

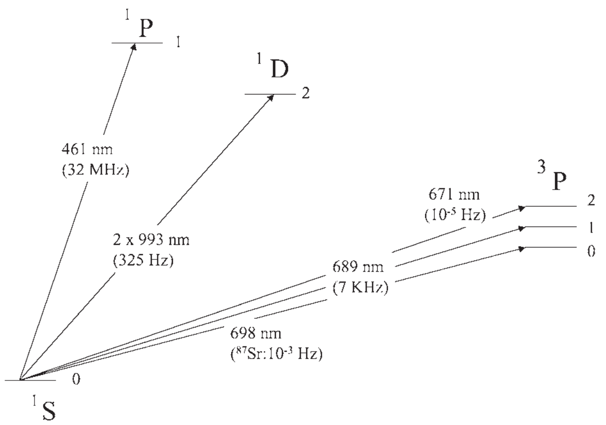

Figure 1: Strontium atomic levels. Except for $^1S_0 \rightarrow {}^3P_0$, linewidths are specified for the boson ^{88}Sr.

Alkaline earth species are prime candidates for optical frequency standards because they can be trapped and cooled on their strong $^1S_0 \rightarrow {}^1P_1$ cycling transition and interrogated using the narrow $^1S_0 \rightarrow {}^3P_1$ intercombination line as the clock transition. Recently, two groups from NIST and PTB have achieved a frequency accuracy close to 10^{-14} with calcium [1]. Strontium is a promising candidate since it has several potential clock transitions and can be simply cooled below 1μK [2, 3]. The cooling process is achieved in two steps: after an efficient capture and pre-cooling using the cycling transition at 461 nm atoms are then transferred to a second trap operating at the intercombination line (689 nm).

For the boson ^{88}Sr, one of the possible clock transitions is the narrow $^1S_0 \rightarrow {}^3P_1$ line with a linewidth of 7.6 kHz. This is the easiest line to investigate, but other resonances have an even smaller linewidth (figure 1). For the fermionic isotope ^{87}Sr, of natural abundance 7%, the $^1S_0 \rightarrow {}^3P_0$ transition is allowed by hyperfine coupling to the levels $^3P_1$ and $^1P_0$. A linewidth of 1 mHz has been estimated using the semiempirical perturbation theory approach by Garstang and constants found in the literature [4, 5, 6]. Furthermore, it seems possible to use a dipole trap in which the $^1S_0$ and the $^3P_0$ states experience equal light shifts, thus leaving the atomic resonance frequency unchanged [7]. Trapped atoms could then be probed in the Lamb-Dicke regime. Such a clock would combine the advantages of both ion and neutral atom clocks.

2 The cold atom source

Figure 2: The cold atom source. From right to left: oven surrounded by two ion pumps, coils of the Zeeman slower (magnetic shield removed), capture region with an other ion pump in a magnetic shield. The total apparatus is one meter long.

The MOT is loaded from an atomic beam shown on figure 2. The oven is heated at about 600°.

Transverse velocity selection is achieved with about a hundred micro-tubes of 8 mm length and 200 μm diameter. This atomic source provides a high flux of atoms: we measured an atomic flux of 2×10^{13} atoms/s. Before entering the capture region the atoms are slowed using a Zeeman slower operating at the $^1S_0 \rightarrow {}^1P_1$ cycling transition at 461 nm.

The atoms are slowed to below the capture velocity of the blue MOT (estimated at 50 m/s) with a Zeeman slower. Numerical simulations have been carried out to maximize the number of slowed atoms in the capture region depending on the magnetic field, the Zeeman length, the laser waist, and the laser power. To minimize the effect of transverse spreading the laser beam is focused with a divergence of 9 mrad. As a result, the saturation parameter varies as the atoms progress into the Zeeman slower, and so too the maximum deceleration:

$$a_{max} = -v_{\rm rec} \frac{\Gamma}{2} \frac{s}{1+s} \qquad (1)$$

where $v_{\rm rec}$ is the recoil velocity, s the saturation parameter and Γ the transition width. Zeeman slowers are usually designed with a constant deceleration $a = \eta\, a_{max}$ where η is smaller than one [8, 9]. In our case, a_{max} is not constant due to focusing. To optimize the efficiency of the slowing process we calculated the magnetic field so as to keep η constant. The obtained magnetic field is show on figure 3.

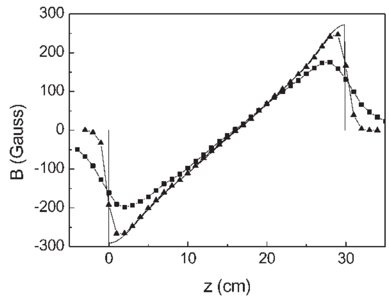

Figure 3: Magnetic field of the Zeeman slower. Continuous line: optimal field computed, ■: field measured without the magnetic shield, ▲: field measured with the magnetic shield around the coils.

The slowing region is 30 cm long. The coils of the Zeeman slower are placed inside a three layer magnetic shield. This minimizes the field perturbation in the MOT region, only 10 cm away from the exit of the Zeeman where the field approaches 30 mT. The shield also provides a sharp field variation at the exit of the slower, which rapidly detunes the atoms with respect to the slowing beam.

The atoms are detected by the fluorescence induced by a probe laser sent at 45°. This beam has a diameter of 2 cm. On figure 4a is shown the velocity distribution of the atom exiting the Zeeman. At an oven temperature of 590°C we measured a maximum of 2.3×10^{11} atoms/s at a velocity lower than 50 m/s. Figure 4b shows the dependence of this number on the power of the Zeeman slower beam. The optimum power is 35 mW, in good agreement with the numerical simulations. At a lower power, only atoms at the center of the gaussian laser beam experience enough deceleration to stay tuned to the laser. On the other hand, at a higher power atoms are slowed to a lower velocity and because of transverse spreading the number of atoms in the capture region decreases.

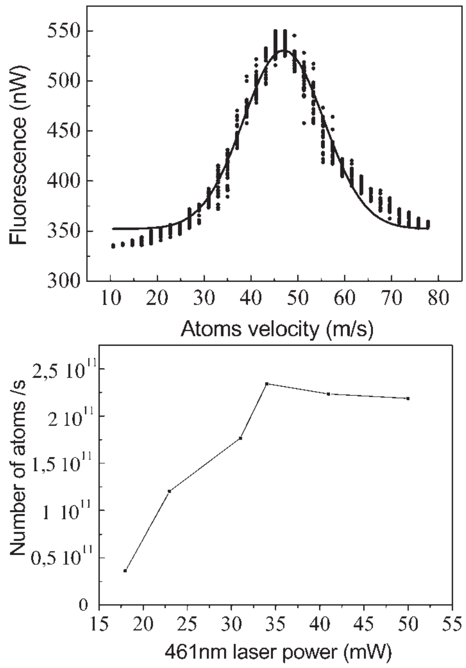

Figure 4: (a) Fluorescence collected in the capture region while sweeping the probe frequency to scan the atomic velocities. The mean velocity of the slowed atoms is 47 m/s. The width (FWHM) of the peak is 17 m/s close to the natural linewidth limited resolution. The power of the beam used for the Zeeman slowing is 34 mW. (b) Number of atoms slowed below 50 m/s in the capture region versus the laser power at 461 nm used for the Zeeman slowing (oven temperature 590°C).

3 Generation of 461 nm light by sum-frequency mixing

To generate the blue light, one possibility is to frequency double a 922 nm laser diode in a $KNbO_3$ crystal [10]. But these diodes are not so common and the $KNbO_3$ crystal leads to high thermal effects. To overcome these problems, we use a sum-frequency mixing of a Nd:YAG at 1064 nm and laser diodes at 813 nm in a KTP crystal [11]. This crystal is far less sensitive to thermal perturbations. The Nd:YAG is a commercial high power device (1.2 W), the power of the 813 nm diodes is 150 mW. We sum the power of two diodes with a 50-50 beam splitter. The measured intracavity power is then doubled.

The crystal is mounted in a ring cavity which has a finesse of respectively 35 and 80 for the 813 nm and the Nd:YAG. The lasers are focused within the crystal with waists of 50μm (813 nm) and 57μm (Nd:YAG). The intracavity power is 2.5 W for the 813 nm and 29 W for the Nd:YAG. With this parameters, we obtained 115 mW of blue power.

On figure 5, right curves show the power reflected by the cavity when spanned over more than a free spectral range. The 813 nm coupling is almost doubled (40% to 70%) when both wavelength are on resonance. This results from an improved impedence matching due to conversion loss [12]. At the same time, the 813 nm power transmitted by the cavity decreases by 45% (left curves on figure 5). Almost 70% of the 813 nm photons coupled into the cavity are converted to blue light.

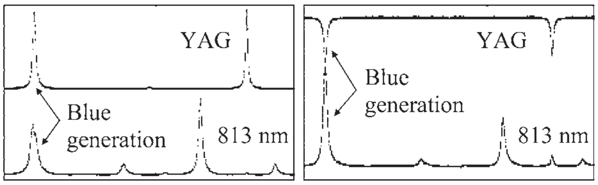

Figure 5: Left curves: transmitted power. Right curves: reflected power.

4 A low frequency noise laser at 689 nm

4.1 Fabry Perot cavity

To provide the ultra-stable laser light at 689 nm an extended cavity laser diode is locked to a high finesse Fabry Perot cavity using the Pound-Drever-Hall technique [13]. Sidebands are generated with a 60 MHz resonant electro-optic modulator. The present bandwidth of the servo control is 2.4 MHz. The cavity, shown in figure 6, has a length L = 10 cm. The spacer is made of ULE. It lies inside a vacuum chamber with three insulations stages to shield it from environmental perturbations. A finesse $F = 28000$ has been measured using the *ring-down technique.* When the laser frequency is swept rapidly across a transmission peak, the transmitted power of the cavity decays exponentially with a time constant τ given by [14]: $\tau = L\,F/\pi c$. The curve is plotted on figure 7.

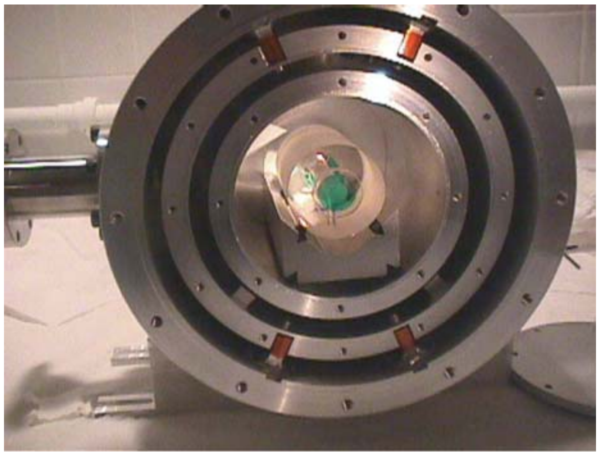

Figure 6: Zerodur cavity in the vacuum chamber.

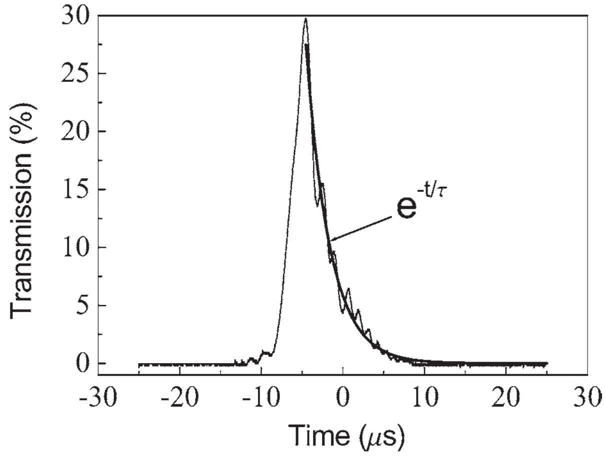

Figure 7: Transmission of the cavity to measure the finesse by the ring down method ($\tau = 2,92\mu s$).

4.2 Ramsey-Bordé interferometer

For long term stabilisation purpose, the 689 nm laser will be locked on the atomic transition using the so-called Ramsey-Bordé interferometer [15]. The atoms experience four $\pi/2$ light pulses that split, deflect, and recombine the atomic wave function. The optical design of this scheme implemented on an atomic beam is shown in figure 8. Each $\pi/2$ pulse is performed with an elliptic beam in order to excite the largest possible proportion of the atoms. It has a waist of 100 μm in the direction of the atomic propagation and of 6 mm in the other direction. The first two interaction beams are reflected by a cat's eye to provide the second pair. This allows the cancellation of the frequency shift due to phase fluctuations induced by the mechanical vibrations of the optical supports. This shift is given by:

$$\delta \propto \phi_2 - \phi_1 - \phi_3 + \phi_4. \qquad (2)$$

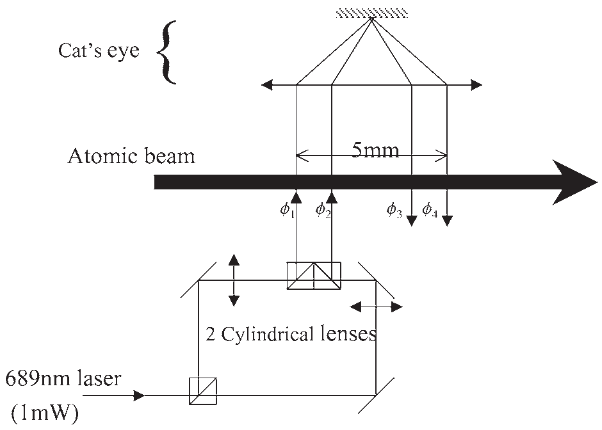

Figure 8: Optical scheme of the Ramsey-Bordé interferometer.

Prospects

With a high power 461 nm laser and a well optimized Zeeman slower, we have been able to slow down more than 2×10^{11} Sr atoms per second. We expect to collect and cool a large number of atoms in a MOT. This will be a key element of a future optical clock using Sr atoms.

References

[1] *Proc. of 6th Symposium on Frequency Standards and Metrology*, P. Gill ed. (World Scientific, Singapore, 2002).

[2] H. Katori *et al.*, Phys. Rev. Lett. **82**, 1116 (1999).

[3] K. Vogel *et al.*, IEEE Trans. on Inst. and Meas. **48**, 618 (1999).

[4] E. Peik *et al.*, Phys. Rev. A, **49**, 402 (1994).

[5] H. Kluge *et al.*, Z. Phys., **270**, 295 (1974).

[6] V. Pal'chikov, in *Proc. of 16th EFTF.*

[7] H. Katori, in *Proc. of 6th Symposium on Frequency Standards and Metrology*, P. Gill ed. (World Scientific, Singapore, 2002).

[8] F. Lison *et al.*, Phys. Rev. A, **61**, 013405 (1999).

[9] P.A. Molenaar *et al.*, Phys. Rev. A, **55**, 605 (1997).

[10] T.P. Dinneen *et al.*, Phys. Rev. A, **59**, 1216 (1999).

[11] W.P. Risk and W.J. Kozlovsky, Opt. Lett., **17**, 707 (1992).

[12] J.D. Vance *et al.*, Appl. Opt., **37**, 4891 (1998).

[13] R.W.P. Drever *et al.*, Phys. B, **31**, 97 (1983).

[14] H.J. Schmitt and H. Zimmer, IEEE Trans. MTT, **14**, 206 (1966).

[15] C.J. Bordé, in *Atom Interferometry*, Paul R. Berman ed., (Academic Press, 1997).